Integration of the Spiral Pulley Negative Stiffness Mechanism into the FishBAC Morphing Wing

Conference Paper · July 2019

6 authors, including:

Chen Wang
Nanjing University of Aeronautics & Astronautics

Jiaying Zhang
Swansea University

Alexander David Shaw
Swansea University

Mohammadreza Amoozgar
University of Hddersfield

IX ECCOMAS Thematic Conference on Smart Structures and Materials
SMART 2019
A. Benjeddou, N. Mechbal and J.F. Deü (Eds)

INTEGRATION OF THE SPIRAL PULLEY NEGATIVE STIFFNESS MECHANISM INTO THE FISHBAC MORPHING WING

C. WANG*, J. ZHANG*, A.D. SHAW*, M. AMOOZGAR*, M.I. FRISWELL* AND B.K.S. WOODS†

*College of Engineering, Swansea University, Swansea, SA1 8EN, UK
Email: chen.wang@swansea.ac.uk

†Department of Aerospace Engineering, University of Bristol, Bristol, BS8 1TR, UK

Key words: Morphing aircraft, Actuation system, Morphing wing, Negative stiffness, Energy balancing

Abstract.

The actuation system of morphing aircraft plays an important role in any promising morphing design. If the structure of the morphing wing needs to be deformed elastically, the actuation system will be required to provide an adequate actuation force while the weight and cost added to the morphing aircraft should be limited to the extent that the performance of the morphing aircraft will not be compromised.

The spiral pulley negative stiffness concept, which uses its stored elastic energy and a negative stiffness mechanism to passively balance the energy requirements of the morphing device, is a promising solution to design the actuation system. The negative stiffness is achieved by the spiral pulley with a spooling cable, which is connected to a pre-stretched spring. The rotation of the spiral pulley can release the energy stored in the spring, and generate the torque to deform the morphing structure. Due to the geometric configuration of the spiral pulley and the kinematic tailoring it provides, negative torque of increasing magnitude is generated as rotation increases, such that the mechanism shows a 'negative stiffness', which will balance the positive stiffness of the morphing structure. Geometry optimisation of the spiral pulley is used to achieve the cancellation. By adopting the negative stiffness mechanism, it is expected that the energy requirement will be balanced, which can significantly reduce the input of external energy and therefore the weight and cost of the actuation system.

In the current study, the spiral pulley negative stiffness mechanism is integrated into a morphing wing employing the Fish Bone Active Camber (FishBAC) morphing concept. The FishBAC wing is actuated by a torque to enable its elastic shape change. The torque requirement to deform the FishBAC wing is measured to identify the positive stiffness. The corresponding negative stiffness is then realised by the optimisation of the geometry configurations of the spiral pulleys, which shows the potential of saving energy of the actuation mechanism.

1 INTRODUCTION

Morphing aircraft have been an important research subject for the last few years. The overall performance of the aircraft can be enhanced by changing the aerodynamic shape actively according to the flight conditions [1-3] .

The idea of changing the aerodynamic shape is not new, indeed it can be traced back to the early period of the aviation age. For example, the wing-warping design was adopted by the Wright brothers' Flyer I for the lateral control [4]. The shape-changing can be achieved through the elastic deformation of the aircraft structure or making use of the novel properties of the smart materials [5, 6], such as the shape memory alloys [7-9] or the piezoelectric materials [10-12] . The wing-warping design is a typical instance of the elastic shape-changing, although it was replaced by the aileron due to the increased flight speeds and the requirement for stiffer structures to avoid aeroelastic failures. The requirement to keep the balance between the flexibility to change shape and the stiffness to carry loads is one of the key factors of a promising morphing aircraft, especially when the weight of the aircraft is also taken in account [13]. A promising morphing aircraft should be capable of changing shape when the aircraft is subject to the corresponding aerodynamic loads, and the morphing structure is usually designed to tailor its stiffness for this purpose.

The actuation system must provide high output force/torque for the minimal system weight, and a high energy efficiency, especially when the shape-changing is achieved by the elastic deformation of the morphing structure. A reduction in actuator mass can potentially be achieved by integrating a negative stiffness mechanism into the structure [14-17]. The negative stiffness mechanism can release the energy stored in a pre-stretched spring and drive the rotation of the spiral pulley, which will provide a negative torque of increasing magnitude against the rotation. The structural stiffness can be balanced by the negative stiffness of the spiral pulley mechanism, which will lead to the zero-stiffness mechanism of the overall system. Since the entire system is balanced and energy is stored in the pre-stretched spring, the energy consumption from external resources can be reduced significantly, which has the potential to reduce the weight of the actuation system and its associated power supply system.

While previous studies have demonstrated this principle in desktop demonstrators [16-18], it has not previously been demonstrated this principle in a true aerodynamic structure. In the current study, the negative stiffness mechanism is integrated into the Fish Bone Active Camber (FishBAC) morphing wing [19-21]. The FishBAC morphing wing is a camber morphing design, which can provide a smooth surface change, and has the potential to increase the lift-to-drag ratio [22, 23]. The shape-changing of FishBAC is generated through the elastic deformation of the bending spine, and servo motors have been adopted to drive the structure. Integration of the negative stiffness mechanism has the potential to improve the performance of the actuation system.

The integration is undertaken in the following steps:

1) Initial wing design: considering the installation of the spiral pulley mechanism;
2) Measurement of the FishBAC structure stiffness;
3) Optimisation of the spiral pulley geometry;
4) Static and wind tunnel test.

In this paper, Section 2 gives a brief discussion of the FishBAC design and the spiral pulley based negative stiffness mechanism. Section 3 discusses the experimental setup to measure the structural stiffness of FishBAC wing, which is used in Section 4 to optimise the geometry of the spiral pulleys, and lays the foundation of the development of a demonstration model.

2 MODEL DEFINITION

Figure 1 shows the schematic of the FishBAC design, which was driven by servo motors [19, 24]. Two tendons are attached to the solid trailing edge section, and the torque generated by the servo motors is transferred onto the spine, which will cause the deformation of the spine. The design, analysis and manufacturing methods have been developed as introduced in the literature and the current study is focused on the integration of the negative stiffness mechanism rather than the FishBAC itself.

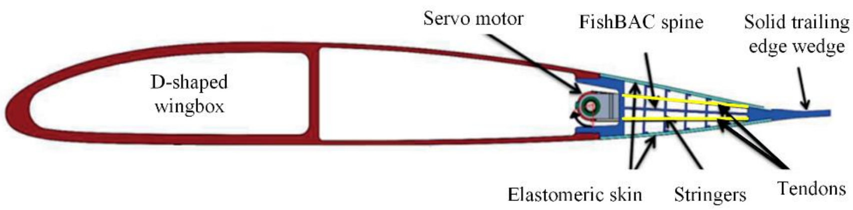

Figure 1: Schematic of FishBAC wing actuated by servo motors [21]

A NACA23012 aerofoil section is selected for the integration, and the chord and span are 270mm and 250mm respectively. One of the difficulties of the integration is the space available in the wing, which is very limited due to the low thickness of the aerofoil. The current approach uses the cable from the load pulley to drive the tendons on the FishBAC directly as shown in Figure 2, which simplifies the mechanism but can still demonstrate the potential of the spiral pulley.

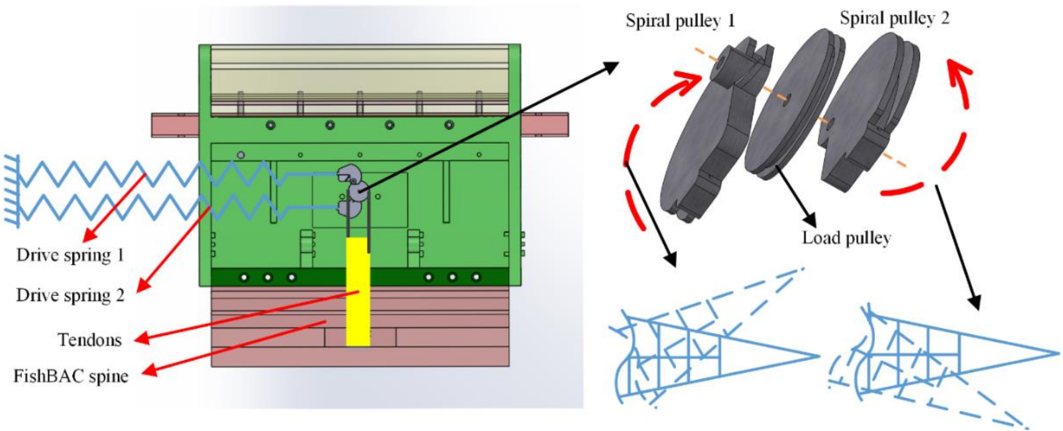

Figure 2: Concept of the integration

The negative stiffness concept used is the bidirectional concept described by Zhang et al. in [17, 18], to assist both positive and negative flap deflections. The drive spring connected to the spiral pulley is pre-stretched with the extension L_0 to store the energy before it is integrated into the wing. If the stiffness rate of the drive spring is denoted as K, the entire energy stored in the drive spring is then $0.5KL_0^2$; this quantifies the maximum amount of available work that can be provided by the mechanism to assist actuation. Two spiral pulleys are mounted onto one centre shaft, and the bidirectional motion can be achieved through the rotation of the pulleys in the opposite directions.

The planar geometry of the spiral pulley is shown in Figure 3.

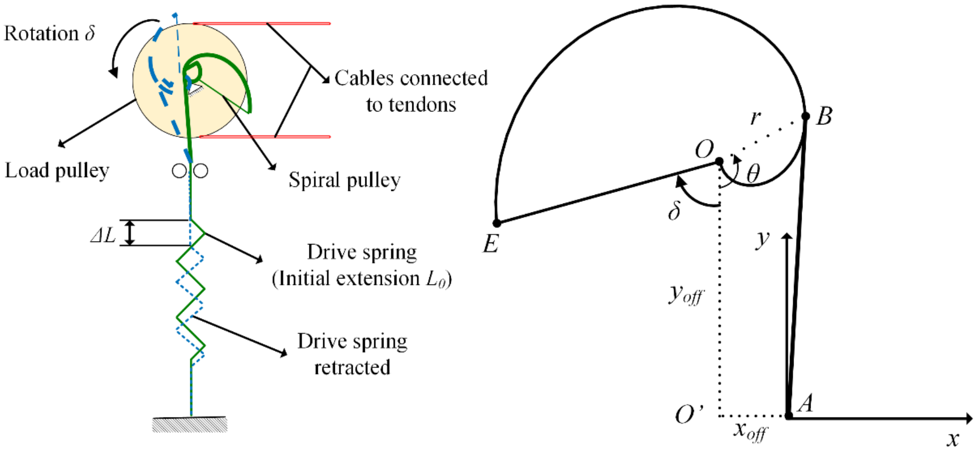

Figure 3: Geometry of the spiral pulley

The radius, r, about point O, which is the centre of the rotation shaft can be defined as an exponential function

$$r = r_o + k_1 e^{k_2(\theta+\delta+\delta_0)} \tag{1}$$

where δ is the rotation angle of the spiral pulley and θ is an associated angle. The parameters k_1, k_2 are the pre-exponent and exponent terms of the spiral pulley. And the coordinate components of point A, x_{off}, y_{off}, are also needed to fully define the pulley geometry, together with the initial pulley radius r_0 and the initial rotation angle δ_0.

The drive torque output by the spiral pulley is given by

$$\begin{aligned} T_d &= F_d l_m \\ F_d &= f(\delta, K, L_0, r_0, \delta_0, k_1, k_2, x_{off}, y_{off}) \\ l_m &= g(\delta, r_0, \delta_0, k_1, k_2, x_{off}, y_{off}) \end{aligned} \tag{2}$$

The expression of the drive torque has been derived in [15, 17]. The force caused by the drive spring, F_d, is determined by the rotation angle, the parameters of the spiral pulley geometry and the drive spring. The moment arm, l_m, also varies with the rotation of the spiral pulley. It can be seen that the drive torque is influenced by the geometry parameters of the spiral pulley and the drive spring stiffness and the initial extension. A decreasing torque can be provided against the rotation of the pulley, which leads to the so-called negative stiffness. In the meantime, the load torque, T_l, is required to deform the structure. If the stiffness of the structure can be balanced by the negative stiffness of the spiral pulley mechanism, a zero-stiffness system can be designed, which means the energy required to deform the structure is provided by the energy stored in the pre-stretched drive springs, and no external energy is needed to deform the structure.

3 STRUCTURE STIFFNESS MEASUREMENT

To design a zero-stiffness mechanism, the relationship between the load torque and the corresponding rotation angle needs to be obtained. The experimental setup is shown in Figure 4. As the focus is the integration of the negative stiffness mechanism, the structure components, including the FishBAC spine, are 3D printed. A baseline load pulley is installed, and the cables from the load pulley are bonded to the tendons of the FishBAC. The baseline load pulley is used to transfer the load torque onto the FishBAC structure in the measurement, and is installed at the same location of the spiral pulley to ensure the integration can be realised. By applying the torque directly onto the load pulley with a torque wrench, the FishBAC spine will be deformed under the specific torque, and the rotation angle is recorded using a protractor.

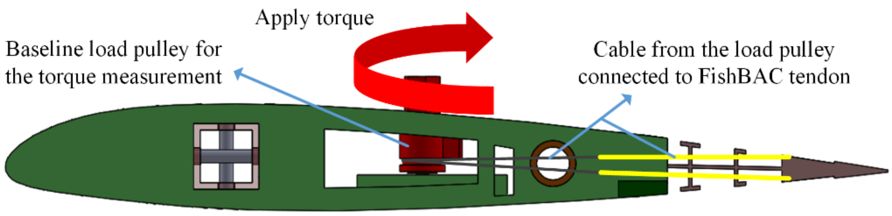

Figure 4: Schematic of the wing platform for the measurement of the FishBAC structure stiffness

As shown in Figure 5(a), both the upward and downward deflections of the FishBAC are achieved. An external load, which is in the opposite direction of the deflection, is applied to on the structure. The relationship between the measured load torque and the rotation angle is shown in Figure 5(b).

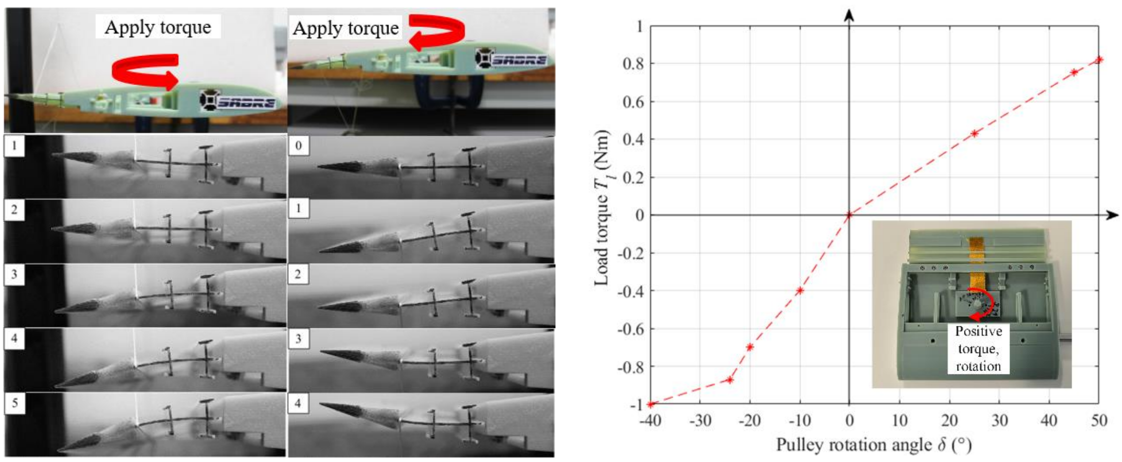

Figure 5: (a) Downward and upward deflection of the FishBAC subject to the load torque, (b) Measured load torque vs the rotation angle of the baseline pulley

The positive torque and rotation angle are defined when they correspond to the upward deflection of the FishBAC tip. It can be seen that the upward and downward deflection of the FishBAC have different stiffnesses, which could be caused by the direction the tendon is aligned, the offset due to the bonding of the tendon, etc. The measurement indicates an approximately linear relationship between the load torque and the rotation angle, although the first data point with the minimum rotation angle is neglected due to measurement errors.

4 OPTIMISATION OF THE SPIRAL PULLEY

To provide a zero-stiffness system, the geometry of the spiral pulley needs to provide the drive torque that can balance the load torque. The geometry parameters are optimised to find the maximum objective defined as

$$\max \eta_e = \frac{E_o}{E_r} \tag{3}$$

where the energy output by the spiral pulley system, E_o, and the energy required by the FishBAC structure, E_r, can be obtained as

$$\begin{aligned} E_o &= \int_0^{\delta} |T_d|\, d\delta \\ E_r &= \int_0^{\delta} |T_l|\, d\delta \end{aligned} \tag{4}$$

The ranges of the variables are given by

$$\begin{cases} -30/1000 \le r_0 \le 10/1000 \text{ (m)} \\ -0.001 \le k_1 \le 0.02 \\ 0 \le k_2 \le 1 \\ -50\pi/180 \le \delta_0 \le 50\pi/180 \\ -0.05 \le L_0 \le 0.4 \text{ (m)} \\ 100 \le K \le 1400 \text{ (N/m)} \\ -0.1 \le x_{off} \le 0.1 \text{ (m)} \\ -0.05 \le y_{off} \le 0.1 \text{ (m)} \end{cases} \tag{5}$$

The Matlab nonlinear programming solver, ‘*fmincon*’, is used to perform the optimisation [25]. Two optimisation cases are performed to find the optimal geometry of the two spiral pulleys for the upward and downward deflections separately, and the optimisation results are summarised in Table 1.

The influence of the spiral pulley on the stiffness is shown in Figure 6. It is found that in both spiral pulleys, the drive torque T_d, can balance the load torque T_l, and the net torque is close to zero, which indicates the zero-stiffness of the mechanism.

Table 1. Optimised parameters of the spiral pulley negative stiffness mechanism

Name of the variable	For the upward deflection	For the downward deflection	Unit
Initial pulley radius r_0	-0.029	-0.030	m
Pre-exponent term k_1	0.005	0.016	
Exponent term k_2	0.991	1.000	
Drive spring extension L_0	0.170	0.218	m
Drive spring rate K	567.153	910.891	N/m
Initial rotation angle of the spiral pulley δ_0	-0.814	-0.758	rad
x coordinate to define point A x_{off}	-0.019	-0.064	m
y coordinate to define point A y_{off}	0.069	0.012	m

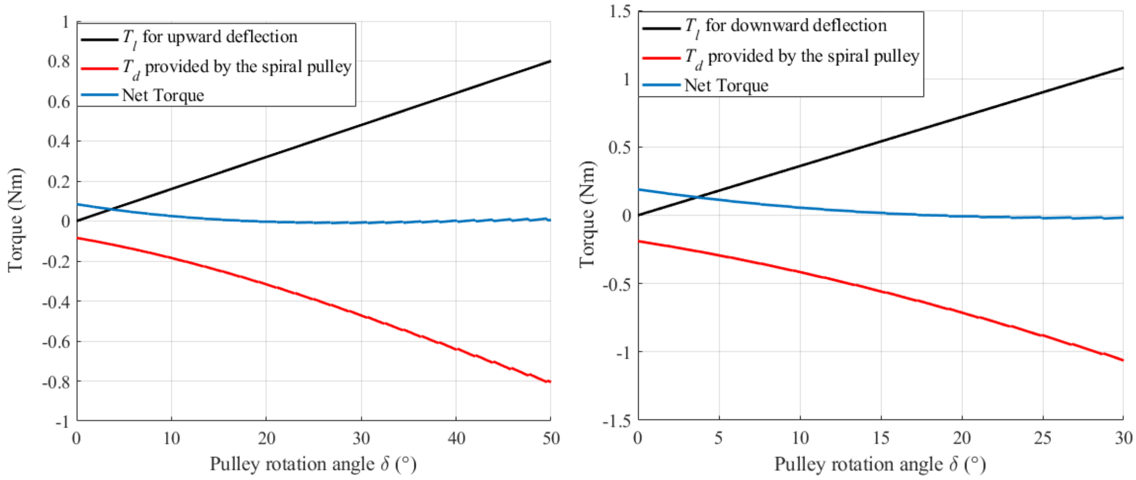

Figure 6: Effect of the optimised spiral pulley on the torque (a) For the upward deflection, (b) For the downward deflection

The influence on the required energy is shown in Figure 7. Obviously, with the spiral pulley mechanism, the external energy, which is required to deform the structure, is reduced significantly, as the energy stored in the pre-stretched spring can drive the mechanism.

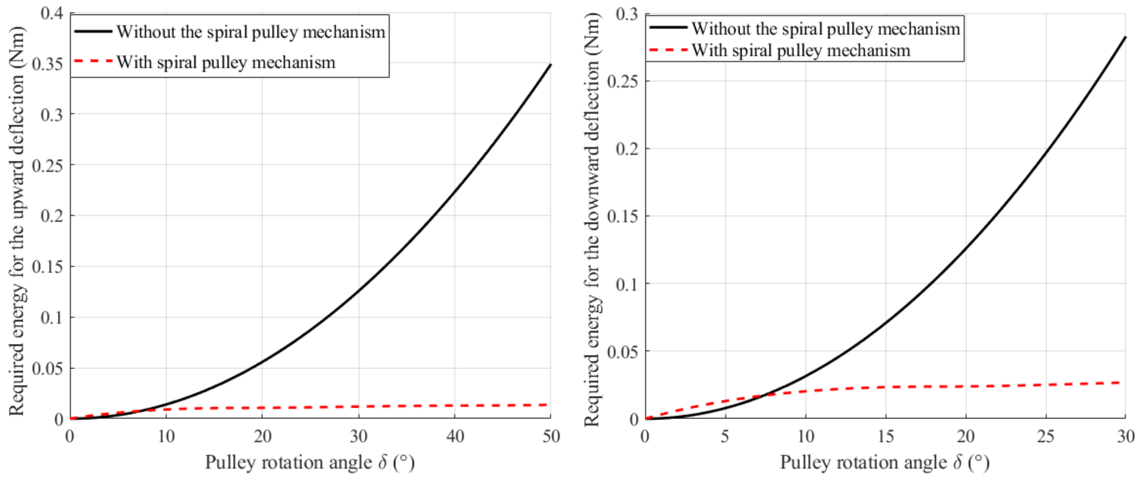

Figure 7: Effect of the optimised spiral pulley on the required energy (a) For the upward deflection, (b) For the downward deflection

5. CONCLUSION

In this paper, the negative stiffness mechanism based on the spiral pulley is integrated into the FishBAC morphing wing.

The load torque, which is required to deform the FishBAC morphing structure, is measured first to obtain the structure stiffness. The geometry parameters of the spiral pulley are then optimised to provide an energy balancing system. The optimisation results indicate that the spiral pulley mechanism is able to provide a negative stiffness against the structure stiffness, which induces a net zero-stiffness of the entire system.

Optimisation work has shown that the spiral pulley is able to provide a high energy efficiency for the morphing structure, and future work will demonstrate a functional model for the static and wind tunnel test.

ACKNOWLEDGEMENTS

The authors acknowledge the financial support provided by the EU H2020 project SABRE, grant agreement 723491.

REFERENCES

1. Barbarino, S., Bilgen, O., Ajaj, R.M., Friswell, M.I., and Inman, D.J., *A review of morphing aircraft.* Journal of Intelligent Material Systems and Structures, 2011. 22(9): p. 823-877.
2. Li, D., Zhao, S., Da Ronch, A., Xiang, J., Drofelnik, J., Li, Y., Zhang, L., Wu, Y., Kintscher, M., Monner, H.P., Rudenko, A., Guo, S., Yin, W., Kirn, J., Storm, S., and Breuker, R.D., *A review of modelling and analysis of morphing wings.* Progress in Aerospace Sciences, 2018. 100: p. 46-62.

3. Weisshaar, T.A., *Morphing aircraft technology-new shapes for aircraft design.* Access number: ADA479821. https://apps.dtic.mil/docs/citations/ADA479821.
4. NASA. *Wing warping*. Available from: https://www.grc.nasa.gov/WWW/Wright/airplane/warp.html.
5. Sun, J., Guan, Q., Liu, Y., and Leng, J., *Morphing aircraft based on smart materials and structures: A state-of-the-art review*. Journal of Intelligent Material Systems and Structures, 2016. 27(17): p. 2289-2312.
6. Thill, C., Etches, J., Bond, I., Potter, K., and Weaver, P., *Morphing skins.* The Aeronautical Journal, 2008. 112(1129): p. 117-139.
7. Chen, S., Chen, Y., Zhang, Z., Liu, Y., and Leng, J., *Experiment and analysis of morphing skin embedded with shape memory polymer composite tube.* Journal of Intelligent Material Systems and Structures, 2014. 25(16): p. 2052-2059.
8. Hartl, D., Lagoudas, D., Calkins, F., and Mabe, J., *Use of a Ni60Ti shape memory alloy for active jet engine chevron application: I. Thermomechanical characterization.* Smart Materials and Structures, 2009. 19(1).
9. Hartl, D., Mooney, J., Lagoudas, D., Calkins, F., and Mabe, J., *Use of a Ni60Ti shape memory alloy for active jet engine chevron application: II. Experimentally validated numerical analysis.* Smart Materials and Structures, 2009. 19(1): p. 015021.
10. Bilgen, O., Kochersberger, K., Diggs, E., Kurdila, A., and Inman, D. *Morphing Wing Micro-Air-Vehicles via Macro-Fiber-Composite Actuators*. *48th AIAA/ASME/ASCE/AHS/ASC Structures, Structural Dynamics, and Materials Conference*. April 23-26, 2007, Honolulu, Hawaii, USA.
11. Bilgen, O., Kochersberger, K.B., and Inman, D.J., *Macro-fiber composite actuators for a swept wing unmanned aircraft.* The Aeronautical Journal, 2009. 113(1144): p. 385-395.
12. Guha, T.K., Oates, W.S., and Kumar, R., *Characterization of piezoelectric macrofiber composite actuated winglets.* Smart Materials and Structures, 2015. 24(6): p. 065043.
13. Campanile, L.F., *Initial Thoughts on Weight Penalty Effects in Shape-adaptable Systems.* Journal of Intelligent Material Systems and Structures, 2005. 16(1): p. 47-56.
14. Woods, B.K.S., Friswell, M.I., and Wereley, N.M., *Advanced Kinematic Tailoring for Morphing Aircraft Actuation.* AIAA Journal, 2014. 52(4): p. 788-798.
15. Woods, B.K. and Friswell, M.I., *Spiral pulley negative stiffness mechanism for passive energy balancing.* Journal of Intelligent Material Systems and Structures, 2016. 27(12): p. 1673-1686.
16. Zhang, J., Shaw, A.D., Amoozgar, M., Friswell, M.I., and Woods, B.K.S., *Bidirectional torsional negative stiffness mechanism for energy balancing systems.* Mechanism and Machine Theory, 2019. 131: p. 261-277.
17. Zhang, J., Shaw, A.D., Mohammadreza, A., Friswell, M.I., and Woods, B.K.S. *Spiral Pulley Negative Stiffness Mechanism for Morphing Aircraft Actuation*. *ASME 2018 International Design Engineering Technical Conferences and Computers and Information in Engineering Conference*. August 26-29, 2018, Quebec City, Quebec, Canada.
18. Zhang, J., Shaw, A.D., Mohammadreza, A., Friswell, M.I., and Woods, B.K.S., *Bidirectional Spiral Pulley Negative Stiffness Mechanism for Passive Energy Balancing.* Journal of Mechanism and Robots, 2019: Accepted, in press.
19. Woods, B.K.S. and Friswell, M.I., *Preliminary Investigation of a Fishbone Active Camber Concept.* 2012(45103): p. 555-563.

20. Woods, B.K., Dayyani, I., and Friswell, M.I., *Fluid/structure-interaction analysis of the fish-bone-active-camber morphing concept.* Journal of Aircraft, 2014. 52(1): p. 307-319.
21. Rivero, A.E., Weaver, P.M., Cooper, J.E., and Woods, B.K.S., *Parametric structural modelling of fish bone active camber morphing aerofoils.* Journal of Intelligent Material Systems and Structures, 2018. 29(9): p. 2008-2026.
22. Woods, B.K., Bilgen, O., and Friswell, M.I., *Wind tunnel testing of the fish bone active camber morphing concept.* Journal of Intelligent Material Systems and Structures, 2014. 25(7): p. 772-785.
23. Woods, B.K.S., Parsons, L., Coles, A.B., Fincham, J.H.S., and Friswell, M.I., *Morphing elastically lofted transition for active camber control surfaces.* Aerospace Science and Technology, 2016. 55: p. 439-448.
24. Rivero, A.E., Fournier, S., Weaver, P.M., Cooper, J.E., and Woods, B.K. *Manufacturing and characterisation of a composite FishBAC morphing wind tunnel model*. *ICAST2018: 29th International Conference on Adaptive Structures and Technologies*. September 30th-October 4th, 2018, Seoul, Korea.
25. Mathworks. *MATLAB*. 2016; Available from: https://uk.mathworks.com/products/global-optimization.html.